
Alleviating Semantic-level Shift: A Semi-supervised Domain Adaptation Method for Semantic Segmentation

Zhonghao Wang
C3SR, UIUC
zhang246@illinois.edu

Yunchao Wei
ReLER, UTS
wychao1987@gmail.com

Rogerio Feris
IBM Research
rsferis@us.ibm.com

Jinjun Xiong
IBM Research
jinjun@us.ibm.com

Wen-Mei Hwu
C3SR, UIUC
w-hwu@illinois.edu

Thomas S. Huang
C3SR, UIUC
t-huang1@illinois.edu

Honghui Shi
C3SR, UIUC
University of Oregon
shihonghui3@gmail.com

Abstract

Learning segmentation from synthetic data and adapting to real data has been extensively studied recently: it can significantly relieve human efforts in labelling pixel-level masks. A key challenge of this task is how to alleviate the data distribution discrepancy between the source and target domains, *i.e.* reducing domain shift. The common approach to this problem is to minimize the discrepancy between feature distributions from different domains through adversarial training. However, directly aligning the feature distribution globally cannot guarantee consistency from a local view (*i.e.* semantic-level), which prevents certain semantic knowledge learned on the source domain from being applied to the target domain. To tackle this issue, we propose a semi-supervised approach named Alleviating Semantic-level Shift (ASS), which can successfully promote the distribution consistency from both global and local views. Specifically, leveraging a small number of labeled data from the target domain, we directly extract semantic-level feature representations from both the source and the target domains by averaging the features corresponding to same categories advised by pixel-level masks. We then feed the produced features to the discriminator to conduct semantic-level adversarial learning, which collaborates with the adversarial learning from the global view to better alleviate the domain shift. We apply our ASS to two domain adaptation tasks, from GTA5 to Cityscapes and from Synthia to Cityscapes. Extensive experiments demonstrate that: (1) ASS can significantly outperform the current unsupervised state-of-the-arts by employing a small number of annotated samples from the target domain; (2) ASS can beat the oracle model trained on the whole target dataset by over 3 points by augmenting the synthetic source data with annotated samples from the target domain without suffering from the prevalent problem of overfitting to the source domain.

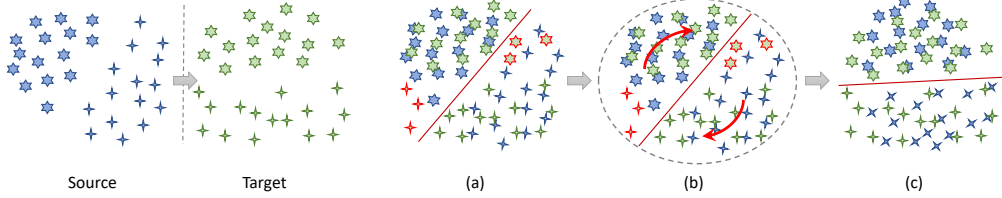


Figure 1: Domain adaptation. (a) Global adaptation. (b) Semantic-level adaptation. (c) Ideal result.

1 Introduction

Due to the development and use of deep learning techniques, major progress has been made in semantic segmentation, one of the most crucial computer vision tasks [2, 3, 34, 4]. However, the current advanced algorithms are often data hungry and require a large amount of pixel-level masks to learn reliable segmentation models. Therefore, one problem arises – *annotating pixel-level masks is costly in terms of both time and money*. For example, Cityscapes [7], a real footage dataset, requires over 7,500 hours of human labor on annotating the semantic segmentation ground truth.

To tackle this issue, unsupervised training methods [6, 24, 25, 33, 27] were proposed to alleviate the burdensome annotating work. Specifically, images labeled from other similar datasets (source domain) can be utilized to train a model and adapted to the target domain by addressing the domain shift issue. For the semantic segmentation task on Cityscapes dataset specifically, previous works [21, 22] have created synthetic datasets which cost little human effort to serve as the source datasets.

While evaluating the previous unsupervised or weakly-supervised methods for semantic segmentation [25, 30, 29, 16, 15, 28], we found that there is still a large performance gap between these solutions and their fully-supervised counterparts. By delving into the unsupervised methods, we observe that the semantic-level features are weakly supervised in the adaptation process and the adversarial learning is only applied on the global feature representations. However, simply aligning the features distribution from global view cannot guarantee consistency in local view, as shown in Figure 1 (a), which leads to poor segmentation performance on the target domain. To address this problem, we propose a semi-supervised learning framework – Alleviating Semantic-level Shift (ASS) model – for better promoting the distribution consistency of features from two domains. In particular, ASS not only adapts global features between two domains but also leverages a few labeled images from the target domain to supervise the segmentation task and the semantic-level feature adaptation task. In this way, the model can ease the inter-class confusion problem during the adaptation process (as shown in Figure 1 (b)) and ultimately alleviate the domain shift from local view (as shown in Figure 1 (c)). As a result, our method 1) is much better than the current state-of-the-art unsupervised methods by using a very small amount of the labeled target domain images; 2) addresses the prevalent problem that semi-supervised models typically overfit to the source domain [26], and outperforms the oracle model trained with the whole target domain dataset by utilizing the synthetic source dataset and labeled images from the target domain.

2 Related works

Semantic segmentation: the semantic segmentation is a challenging computer vision task. Ever since the surge of deep learning methods, the state of the art of this task has been raised by a large amount. Deeplab [2–4] is such a series of deep learning models that attained top on the 2017 Pascal VOC [9] semantic segmentation challenge. It uses Atrous Spatial Pyramid Pooling (ASPP) module which combines multi-rate atrous convolutions and the global pooling technique to enlarge the field of view on the feature map and therefore deepen the model’s understanding of the global semantic context. Deeplab v2 has laconic structure and good performance in extracting images features and can be easily trained. Therefore, it is selected as the backbone network for our work.

Domain adaptation: It is very expensive to collect and annotate datasets for a specific task. However, there are many relative datasets for other tasks available in today’s big data era [26]. Thus, we can transfer and apply the useful knowledge of the model trained on the off-the-shelf dataset to the target task [10]. A typical structure for domain adaptation is Generative Adversarial Networks (GAN)

[11]. This model trains a generative network and a discriminative network in an adversarial strategy. That is, the discriminative network is updated to distinguish which domain the input feature map is from, while the generative network generates the feature map to fool the discriminative network. The discriminative network will thereby supervise the generative network to minimize the discrepancy of the feature representations from the two domains. As a result, The model can apply the knowledge learned from the source domain to the task on the target domain.

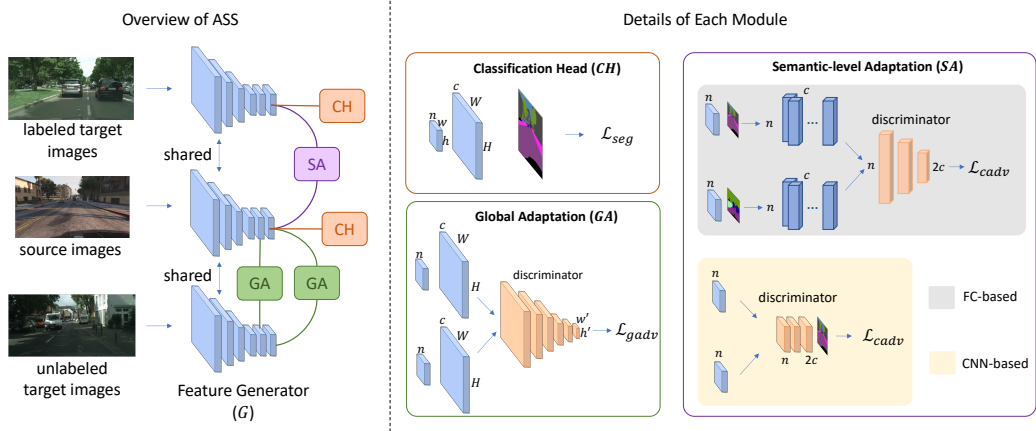


Figure 2: Structure overview. c is the number of classes for adaptation. W and H are the width and height of the input image respectively. n is the number of feature channels of the feature map.

3 Method: Alleviating Semantic-level Shift

3.1 Overview of the Model Structure

We randomly select a subset of images from the target domain with ground truth annotations, and denote this set of images as $\{\mathcal{I}_{\mathcal{T}_c}\}$. We denote the whole set of source images and the set of unlabeled target images as $\{\mathcal{I}_S\}$ and $\{\mathcal{I}_{\mathcal{T}_u}\}$ respectively. As shown in Figure 2, our domain adaptation structure has four modules: the feature generation module G , the segmentation classification module CH , the global feature adaptation module GA and the semantic-level adaptation module SA . We denote the output feature maps of G by F , the ground truth label maps by Y and the downsampled label maps (of the same height and width as F) as y . We use H, W to denote the height and width of the input image, h, w to denote those of F , and h', w' to denote those of the confidence maps output by the discriminator of GA . C is the class set, c is the number of classes, and n is the channel number of F .

When testing the model, we forward the input image to G and use CH to operate on F to predict the semantic class that each pixel belongs to. The following sections will introduce the details of each module.

3.2 Segmentation

We forward F to a convolutional layer to output the score maps with c channels. Then, we use a bilinear interpolation to upsample the score maps to the original input image size and apply a softmax operation channel-wisely to get score maps P . The segmentation loss L_{seg} is calculated as

$$L_{seg}(I) = - \sum_{H,W} \sum_{k \in C} Y^{(H,W,k)} \log(P^{(H,W,k)}) \quad (1)$$

3.3 Global Feature Adaptation Module

This module adapts F from the source domain to the target domain. we input the source image score maps P_s to the discriminator D_g of GA to conduct the adversarial training. We define the adversarial loss as:

$$L_{gadv}(I_s) = - \sum_{h',w'} \log(D_g(P_s)^{(h',w',1)}) \quad (2)$$

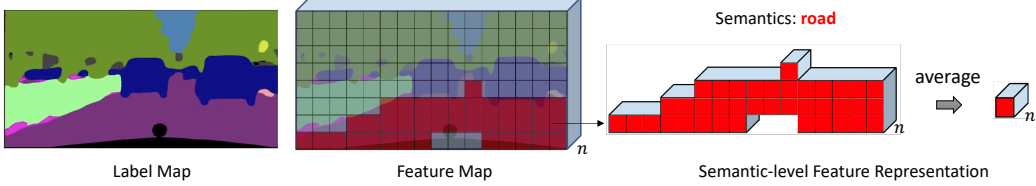


Figure 3: Feature vector generation for the fully connected class feature adaptation. This example generates the feature vector for the class road. We first resize the ground truth label maps to the size of the feature maps; then, align them with the feature maps and find the locations of the class feature vectors shown in red color; crop these feature vectors and average across the height and width to get the averaged feature vector of a certain class.

We define 0 as the source domain pixel and 1 as the target domain pixel for the output of D_g . Therefore, this loss will force G to generate features closer to the target domain globally. To train D_g , we forward P_s and P_{t_u} to D_g in sequence. The loss of D_g is calculated as:

$$L_{gd}(P) = - \sum_{h',w'} ((1 - z) \log(D_g(P_s)^{(h',w',0)}) + z \log(D_g(P_t)^{(h',w',1)})) \quad (3)$$

where $z = 0$ if the feature maps are from the source domain and $z = 1$ if the feature maps are from the target domain.

3.4 Semantic-level adaptation module

This module adapts the feature representation for each class in the source domain to the corresponding class feature representation in the target domain to alleviate the domain shift from semantic-level.

3.4.1 Fully connected semantic-level adaptation

We believe that the feature representation for a specific class at each pixel should be close to each other. Thereby, we can average these feature vectors across the height and width to represent the semantic-level feature distribution, and adapt the averaged feature vectors to minimize the distribution discrepancy between two domains. As shown in Figure 3, the semantic-level feature vector V_k of class k is calculated as

$$V^k = \frac{\sum_{h,w} y^{(h,w,k)} F^{(h,w,:)}}{\sum_{h,w} y^{(h,w,k)}} \quad (4)$$

where $k \in C$, $V^k \in \mathbb{R}^n$. Then we forward these semantic-level feature vectors to the semantic-level feature discriminator D_s for adaptation, as shown in Figure 2. D_s only has 2 fully connected layers, and outputs a vector of $2c$ channels after a softmax operation. The first half and the last half channels correspond to classes from the source domain and the target domain respectively. Therefore, the adversarial loss can be calculated as

$$L_{sadv}(I_s) = - \sum_{k \in C} \log(D_s(V_s^k)^{(k+c)}) \quad (5)$$

To train D_s , we let it classify the semantic-level feature vector to the correct class and domain. The loss of D_s can be calculated as:

$$L_{sd}(V) = - \sum_{k \in C} ((1 - z) \log(D_s(V^k)^{(k)}) + z \log(D_s(V^k)^{(k+c)})) \quad (6)$$

where $z = 0$ if the feature vector is from the source domain and $z = 1$ if it is from the target domain.

3.4.2 CNN semantic-level feature adaptation

We observe that it is hard to extract the semantic-level feature vectors, because we have to use the label maps to filter pixel locations and generate the vectors in sequence. Therefore, inspired from the previous design, we come up with a laconic CNN semantic-level feature adaptation module. The discriminator uses convolution layers with kernel size 1×1 , which acts as using the fully connected

discriminator to operate on each pixel of F , as shown in Figure 2. The output has $2c$ channels after a softmax operation where the first half and the last half correspond to the source domain and the target domain respectively. Then, the adversarial loss can be calculated as:

$$L_{sadv}(I_s) = - \sum_{h,w} \log(D_s(F_s)^{(h,w,k+c)}) \quad (7)$$

where k is the pixel ground truth class. To train the discriminator, we can use the loss as follows:

$$L_{sd}(F) = - \sum_{h,w} ((1-z) \log(D_s(F)^{(h,w,k)}) + z \log(D_s(F)^{(h,w,k+c)})) \quad (8)$$

3.5 Adversarial learning procedure

Our ultimate goal for G is to have a good semantic segmentation ability by adapting features from the source domain to the target domain. Therefore, the training objective for G can derive from Eqn (1) as

$$L(I_s, I_{t_l}) = \lambda_{seg}(L_{seg}(I_s) + L_{seg}(I_{t_l})) + \lambda_{gadv}L_{gadv}(I_s) + \lambda_{sadv}L_{sadv}(I_s) \quad (9)$$

where λ is the weight parameter. The two discriminators should be able to distinguish which domain the feature maps are from, which enables the features to be adapted in the right direction. We can simply sum up the two discriminator losses as the training objective for discriminative modules.

$$L(F_s, F_{t_u}, F_{t_l}) = \lambda_{gd}(L_{gd}(F_s) + L_{gd}(F_{t_u})) + \lambda_{sd}(L_{sd}(F_s) + L_{sd}(F_{t_l})) \quad (10)$$

In summary, we will optimize the following min-max criterion to let our model perform better in segmentation task by adapting the features extracted from the source domain more alike the ones extracted from the target domain.

$$\max_{D_g, D_s} \min_G L(I_s, I_{t_l}) - L(F_s, F_{t_u}, F_{t_l}) \quad (11)$$

4 Implementation

4.1 Network Architecture

Segmentation Network. We adopt ResNet-101 model [12] pre-trained on ImageNet [8] with only the 5 convolutional layers $\{conv1, res2, res3, res4, res5\}$ as the backbone network. Due to memory limit, we do not use the multi-scale fusion strategy [32]. For generating better-quality feature maps, we follow the common practice from [2, 32, 25] and twice the resolution of the feature maps of the final two layers. To enlarge the field of view, we use dilated convolutional layers [32] with stride 2 and 4 in $res4$ and $res5$. For the classification heads, we apply two ASPP modules [3] to $res4$ with $\lambda_{seg1} = 0.1$ and $res5$ with $\lambda_{seg2} = 1$ respectively. With upsampling the output of $res5$ and a softmax operation, our backbone model achieves 65.91 mIoU scores with a fully-supervised scheme which is similar to the performance reported in [25].

Global Discriminator. Following [25], We use 5 convolutional layers with kernel size 4×4 , stride of 2 and channel number of $\{64, 128, 256, 512, 1\}$ respectively to form the network. We use a leaky ReLU [19] layer of 0.2 negative slope between adjacent convolutional layers. Due to the small batch size in the training process, we do not use batch normalization layers [17]. Two independent global discriminators are used for $res4$ with $\lambda_{gadv1} = 0.0002$ and $res5$ with $\lambda_{gadv2} = 0.001$.

Fully Connected semantic-level Discriminator. We use two fully connected layers with channel number of 1024 and twice the class number respectively, and we put a Leaky ReLU [19] of 0.2 negative slope between them.

CNN Semantic-level Discriminator. We use two convolutional layers with the kernel size of 1×1 , stride of 1 and channel number of 1024 and twice the class number respectively. We insert a Leaky ReLU [19] layer with 0.2 negative slope between the two convolutional layers.

4.2 Network Training

We train the network with two stages. First, we train the segmentation network with GA until convergence. Then, we use the $GA + SA$ to refine the training process. At the first stage, for

Table 1: Results of adapting GTA5 to Cityscapes. The first four rows show the performance of the current state-of-the-art unsupervised algorithms. The following row shows the performance of our segmentation network trained on the whole Cityscapes dataset. The last six rows show the performance of our models trained with different number of Cityscapes labeled images.

Method	GTA5 → Cityscapes																			
	road	sidewalk	building	wall	fence	pole	light	sign	vegetation	terrain	sky	person	rider	car	truck	bus	train	motorbike	bike	mIoU
Wu et al.[31]	85.0	30.8	81.3	25.8	21.2	22.2	25.4	26.6	83.4	36.7	76.2	58.9	24.9	80.7	29.5	42.9	2.5	26.9	11.6	41.7
Tsai et al.[25]	86.5	36.0	79.9	23.4	23.3	23.9	35.2	14.8	83.4	33.3	75.6	58.5	27.6	73.7	32.5	35.4	3.9	30.1	28.1	42.4
Saleh et al.[23]	79.8	29.3	77.8	24.2	21.6	6.9	23.5	44.2	80.5	38.0	76.2	52.7	22.2	83.0	32.3	41.3	27.0	19.3	27.7	42.5
Hong et al.[14]	89.2	49.0	70.7	13.5	10.9	38.5	29.4	33.7	77.9	37.6	65.8	75.1	32.4	77.8	39.2	45.2	0.0	25.5	35.4	44.5
oracle wholecity	96.7	75.7	88.3	46.0	41.7	42.6	47.9	62.7	88.8	53.5	90.6	69.1	49.7	91.6	71.0	73.6	45.3	52.0	65.5	65.9
ours+50city	94.3	63.0	84.5	26.8	28.0	38.4	35.5	48.7	87.1	39.2	88.8	62.2	16.3	87.6	23.2	39.2	7.2	24.4	58.1	50.1
ours+100city	96.0	71.7	85.9	27.9	27.6	42.8	44.7	55.9	87.7	46.9	89.0	66.0	36.4	88.4	28.9	21.4	11.4	38.0	63.2	54.2
ours+200city	96.1	71.9	85.8	28.4	29.8	42.5	45.0	56.2	87.4	45.0	88.7	65.8	38.2	89.6	42.2	35.9	17.1	35.8	61.6	56.0
ours+500city	96.2	72.7	87.6	35.1	31.7	46.6	46.9	62.7	88.7	49.6	90.5	69.2	42.7	91.1	52.6	60.9	9.6	43.1	65.6	60.2
ours+1000city	96.8	76.3	88.5	30.5	41.7	46.5	51.3	64.3	89.1	54.2	91.0	70.7	48.7	91.6	59.9	68.0	40.8	48.0	67.0	64.5
ours+2975city(all)	97.3	79.3	89.8	47.4	49.7	48.9	52.9	67.4	89.7	56.3	91.9	72.2	53.1	92.6	69.3	78.4	58.0	51.2	68.2	69.1

Table 2: GTA5 → Cityscapes: performance contributions of adaptation modules. The oracle model is only trained with the given number of Cityscapes labeled images. FCSA: Fully connected semantic-level feature adaptation module. CSA: CNN semantic-level feature adaptation module. We present the improvements of the model *GA + CSA* over the oracle model.

# of Cityscapes images	Oracle	GA	GA+FCSA	GA+CSA	Improvements
0	-	42.37	-	-	-
50	39.47	49.98	50.16	50.13	+10.66
100	43.55	53.45	54.11	54.21	+10.66
200	47.12	54.37	56.35	55.95	+8.83
500	53.58	56.45	59.89	60.16	+6.58
1000	58.61	57.96	63.80	64.47	+5.86
2975 (all)	65.91	59.71	68.84	69.14	+3.23

one iteration, we forward I_s and I_{t_l} to G and optimize L_{seg} ; then, we pass generated P_s to GA to optimize L_{gadv} ; After that, we forward I_{t_u} to G to generate P_{t_u} ; we finally use P_{t_u} along with P_s to optimize L_{gd} . At the second stage, besides all the training strategy in the first stage, when forwarding I_s and I_{t_l} to G , we also optimize G for L_{sadv} ; at the final step, we also use F_s and F_{t_l} to optimize SA for L_{sd} .

We use Pytorch toolbox and a single NVIDIA V100 GPU with 16 GB memory to train our network. Stochastic Gradient Descent (SGD) is used to optimize the segmentation network. We use Nesterov’s method [1] with momentum 0.9 and weight decay 5×10^{-4} to accelerate the convergence. Following [2], we set the initial learning rate to be 2.5×10^{-4} and let it polynomially decay with the power of 0.9. We use Adam optimizer [18] with momentum 0.9 and 0.99 for all the discriminator networks. We set the initial learning rate to be 10^{-4} and follow the same polynomial decay rule.

5 Experiments

We validate the effectiveness of our proposed method by transferring our model trained with synthetic datasets (i.e., GTA5 [21] and SYNTHIA [22]) in a semi-supervised setting to test on the real-world image dataset Cityscapes [7].

Table 3: Global adaptation direction comparison

# of Cityscapes images	source→target	source←target	source↔target
50	49.98	45.80	44.50
100	53.45	49.92	49.09
200	54.37	52.85	51.82
500	56.45	55.78	52.10

Table 4: parameters analysis

# of Cityscapes images	$\lambda = 1$	$\lambda = 0.2$	$\lambda = 0.04$	$\lambda = 0.008$	$\lambda = 0.001$
100	54.11	53.87	53.68	53.96	53.92
500	59.76	59.29	59.89	59.74	59.69

(a): λ_{sadv} for fully connected semantic-level adaptation module					
# of Cityscapes images	$\lambda = 1$	$\lambda = 0.1$	$\lambda = 0.01$	$\lambda = 0.001$	
500	59.76	59.46	60.16	59.67	

(b): λ_{sadv} for CNN semantic-level adaptation module					
--	--	--	--	--	--

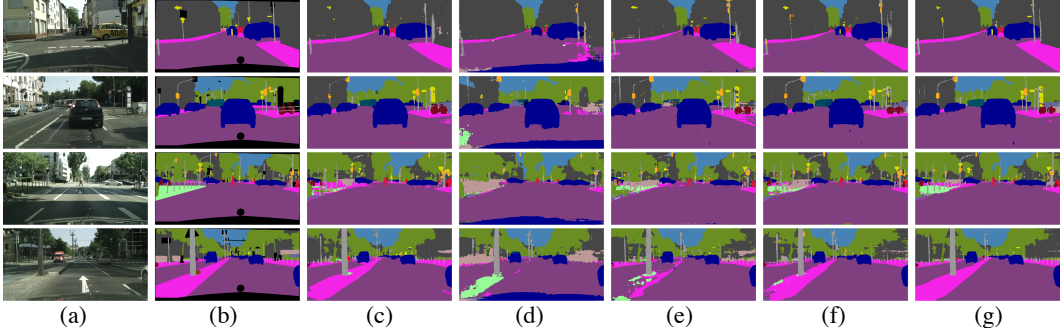


Figure 4: (a) image; (b) ground truth; (c) oracle model trained with the whole Cityscapes dataset; (d) unsupervised; (e) ours+200city; (f) ours+1000city; (g) ours+wholecity

5.1 Datasets

The Cityscapes [7] dataset consists of 5000 images of resolution 2048×1024 with high-quality pixel-level annotations. These images of street scenes were annotated with 19 semantic labels for evaluation. This dataset is split into training, validation and test sets with 2975, 500 and 1525 images respectively. Following previous works [13, 20], We only evaluate our models on the validation set. The GTA5 [21] dataset contains 24966 fine annotated synthetic images of resolution 1914×1052 . All the images are frames captured from the game Grand Theft Auto V. This dataset shares all the 19 classes used for evaluation in common with the Cityscapes dataset. The SYNTHIA [22] dataset has 9400 images of resolution 1280×760 with pixel-level annotations. Similar to [5, 25], we evaluate our models on Cityscapes validation set with the 13 classes shared in common between SYNTHIA dataset and Cityscapes dataset.

5.2 GTA5

We present the result of adapting our model from GTA5 dataset to Cityscapes dataset in Table 1. For fairness, We compare our results with the current state-of-the-art unsupervised algorithms using ResNet-101 [12] as the backbone structure. As a result, our semi-supervised model trained with a few labeled Cityscapes data (e.g. 50 images) can beat all the unsupervised models; if trained with 1000 labeled Cityscapes images, it can achieve a performance close to that of the oracle model; if trained with the whole labeled Cityscapes dataset, it outperforms the oracle model by 3.2 points of mIoU. This result addresses the issue that a semi-supervised model easily overfits to the source domain dataset [26]. We provide some visualization results in Figure 4.

Then, we do ablation studies on the performance contribution of each adaptation module. The result is shown in Table 2. First, the contribution of *GA* module disappears or is negative when the labeled Cityscapes images reach a number of 1000 or more. Compared to the model with only *GA* module, the models *GA + FCSA* and *GA + CSA* both have on-par improvements if trained with over 50 Cityscapes labeled images. Due to a simpler structure, we report the performance improvements of the model *GA + CSA* over the oracle model in Table 2, and this model is recommended for the semantic-level adaptation.

We conjecture that the *SA* module adaptation direction should follow the *GA* one, or it would lead to a bad performance. Therefore, we experiment on which adaptation direction the model with *GA* module can achieve the optimal result. As shown in Table 3, the model adapted from the source domain to the target domain always achieves the best performance. Therefore, we let all of our adaptation modules follow this adaptation direction.

Table 5: Results of adapting SYNTHIA to Cityscapes. The first three rows show the performance of the current state-of-the-art unsupervised algorithms. The following row shows the performance of our segmentation network trained on the whole Cityscapes dataset. The last six rows show the performance of our models trained with different number of Cityscapes labeled images.

Method	SYNTHIA → Cityscapes													
	road	sidewalk	building	light	sign	vegetation	sky	person	rider	car	bus	motorbike	bike	mIoU
Wu et al.[31]	81.5	33.4	72.4	8.6	10.5	71.0	68.7	51.5	18.7	75.3	22.7	12.8	28.1	42.7
Tsai et al.[25]	84.3	42.7	77.5	4.7	7.0	77.9	82.5	54.3	21.0	72.3	32.2	18.9	32.3	46.7
Hong et al.[14]	85.0	25.8	73.5	19.5	21.3	67.4	69.4	68.5	25.0	76.5	41.6	17.9	29.5	47.8
oracle wholecity	96.5	77.6	91.2	49.0	62.1	91.4	90.2	70.1	47.7	91.8	74.9	50.1	66.9	73.8
ours+50city	94.1	63.9	87.6	18.1	37.1	87.5	89.7	64.6	37.0	87.4	38.6	23.2	59.6	60.7
ours+100city	93.6	64.6	88.8	30.4	43.3	89.0	89.2	65.3	25.1	88.2	47.4	23.8	59.2	62.1
ours+200city	95.2	71.2	89.1	32.9	46.4	89.1	90.3	67.0	31.6	89.4	42.3	32.9	64.8	64.8
ours+500city	96.7	77.1	91.0	42.6	62.2	91.2	91.3	69.5	34.8	91.6	56.3	35.0	68.0	69.8
ours+1000city	97.2	80.6	91.3	46.3	66.4	91.5	91.4	71.6	45.0	92.2	61.5	45.3	68.4	73.0
ours+2975city(all)	97.5	82.7	92.4	53.3	69.7	92.2	92.8	73.6	52.4	93.7	79.3	50.9	71.5	77.1

Table 6: SYNTHIA → Cityscapes: performance contributions of adaptation modules. We present the improvements of the better model between *GA* and *GA + CSA* over the oracle model.

# of Cityscapes images	Oracle	GA	GA+CSA	Improvements
0	-	46.74	-	-
50	52.62	60.65	57.37	+8.03
100	57.59	62.14	58.34	+4.55
200	60.84	64.79	64.47	+3.95
500	66.54	69.07	69.79	+3.25
1000	70.70	71.80	72.97	+2.27
2975 (all)	73.80	74.97	77.08	+3.28

In Table 4, we analyse how the selection of λ_{sadv} affects the performance of our model. Due to our two-stage training method, the first stage serves as a warm-up procedure for the second one. Thus, either the *FCSA* module or the *CSA* module is insensitive to the selection of λ_{sadv} . For the best performance, we choose λ_{sadv} to be 1 for the *FCSA* module and 0.01 for *CSA* module.

5.3 SYNTHIA

We present the result of adapting our model from SYNTHIA to Cityscapes in Table 5. Again, our model with a few labeled Cityscapes images can beat the unsupervised methods with a large margin; it can compete with the oracle model with around 1000 labeled Cityscapes images; it outperforms the oracle model by 3.3 points in mIoU with the whole labeled Cityscapes images.

We conduct ablation studies on the adaptation module contributions as shown in Table 6. The contribution of *GA* module decreases as the number of supervised Cityscapes images increases. The *GA + CSA* model is worse than the model with only *GA* module with fewer than 500 labeled Cityscapes images, but it is better with no fewer than 500 labeled Cityscapes images. We conjecture that if the randomly selected labeled Cityscapes images cannot represent the whole Cityscapes semantic-level feature distribution, the *SA* module cannot adapt the semantic-level features in an appropriate direction, and thus leads to an inferior performance. Further researches can be done to address how to select target domain labeled images which makes the adaptation more meaningful.

6 Conclusion

This paper proposes a semi-supervised learning framework to adapt the global feature and the semantic-level feature from the source domain to the target domain for the semantic segmentation task. As a result, with a few labeled target images, our model outperforms current state-of-the-art unsupervised models by a great margin. Our model can also beat the oracle model trained on the whole dataset from target domain by utilizing the synthetic data with the whole target domain labeled images without suffering from the prevalent problem of overfitting to the source domain.

References

- [1] Aleksandar Botev, Guy Lever, and David Barber. Nesterov’s accelerated gradient and momentum as approximations to regularised update descent. In *IEEE IJCNN*, pages 1899–1903, 2017.
- [2] Liang-Chieh Chen, George Papandreou, Iasonas Kokkinos, Kevin Murphy, and Alan L Yuille. Semantic image segmentation with deep convolutional nets and fully connected crfs. *arXiv preprint arXiv:1412.7062*, 2014.
- [3] Liang-Chieh Chen, George Papandreou, Iasonas Kokkinos, Kevin Murphy, and Alan L Yuille. Deeplab: Semantic image segmentation with deep convolutional nets, atrous convolution, and fully connected crfs. *IEEE TPAMI*, 40(4):834–848, 2017.
- [4] Liang-Chieh Chen, George Papandreou, Florian Schroff, and Hartwig Adam. Rethinking atrous convolution for semantic image segmentation. *arXiv preprint arXiv:1706.05587*, 2017.
- [5] Yi-Hsin Chen, Wei-Yu Chen, Yu-Ting Chen, Bo-Cheng Tsai, Yu-Chiang Frank Wang, and Min Sun. No more discrimination: Cross city adaptation of road scene segmenters. In *IEEE ICCV*, 2017.
- [6] Yuhua Chen, Wen Li, and Luc Van Gool. Road: Reality oriented adaptation for semantic segmentation of urban scenes. In *IEEE CVPR*, 2018.
- [7] Marius Cordts, Mohamed Omran, Sebastian Ramos, Timo Rehfeld, Markus Enzweiler, Rodrigo Benenson, Uwe Franke, Stefan Roth, and Bernt Schiele. The cityscapes dataset for semantic urban scene understanding. In *IEEE CVPR*, 2016.
- [8] Jia Deng, Wei Dong, Richard Socher, Li-Jia Li, Kai Li, and Li Fei-Fei. Imagenet: A large-scale hierarchical image database. In *IEEE CVPR*, 2009.
- [9] Mark Everingham, S. M. Ali Eslami, Luc Van Gool, Christopher K. I. Williams, John Winn, and Andrew Zisserman. The pascal visual object classes challenge: A retrospective. *IJCV*, 111(1):98–136, 2015.
- [10] Yaroslav Ganin, Evgeniya Ustinova, Hana Ajakan, Pascal Germain, Hugo Larochelle, François Laviolette, Mario Marchand, and Victor Lempitsky. Domain-adversarial training of neural networks. *JMLR*, 17(1):2096–2030, 2016.
- [11] Ian J. Goodfellow, Jean Pouget-Abadie, Mehdi Mirza, Bing Xu, David Warde-Farley, Sherjil Ozair, Aaron Courville, and Yoshua Bengio. Generative Adversarial Networks. *NIPS*, 2014.
- [12] Kaiming He, Xiangyu Zhang, Shaoqing Ren, and Jian Sun. Deep residual learning for image recognition. In *IEEE CVPR*, 2016.
- [13] Judy Hoffman, Dequan Wang, Fisher Yu, and Trevor Darrell. Fcns in the wild: Pixel-level adversarial and constraint-based adaptation. *arXiv preprint arXiv:1612.02649*, 2016.
- [14] Weixiang Hong, Zhenzhen Wang, Ming Yang, and Junsong Yuan. Conditional generative adversarial network for structured domain adaptation. In *IEEE CVPR*, 2018.
- [15] Qibin Hou, PengTao Jiang, Yunchao Wei, and Ming-Ming Cheng. Self-erasing network for integral object attention. In *NIPS*, 2018.
- [16] Zilong Huang, Xinggang Wang, Jiasi Wang, Wenyu Liu, and Jingdong Wang. Weakly-supervised semantic segmentation network with deep seeded region growing. In *IEEE CVPR*, 2018.
- [17] Sergey Ioffe and Christian Szegedy. Batch normalization: Accelerating deep network training by reducing internal covariate shift. In *ICML*, 2015.
- [18] Diederik P. Kingma and Jimmy Ba. Adam: A Method for Stochastic Optimization. In *ICLR*, 2014.
- [19] Andrew L. Maas, Awni Y Hannun, and Andrew Ng. Rectifier nonlinearities improve neural network acoustic models. In *ICML*, 2013.

[20] Xingchao Peng, Ben Usman, Neela Kaushik, Judy Hoffman, Dequan Wang, and Kate Saenko. VisDA: The Visual Domain Adaptation Challenge. *arXiv preprint arXiv:1710.06924*, 2017.

[21] Stephan R. Richter, Vibhav Vineet, Stefan Roth, and Vladlen Koltun. Playing for data: Ground truth from computer games. In *ECCV*, 2016.

[22] German Ros, Laura Sellart, Joanna Materzynska, David Vazquez, and Antonio Lopez. The SYNTHIA Dataset: A large collection of synthetic images for semantic segmentation of urban scenes. In *IEEE CVPR*, 2016.

[23] Fatemeh Saleh, Sadegh Aliakbarian, Mathieu Salzmann, Lars Petersson, and Jose M. Alvarez. Effective use of synthetic data for urban scene semantic segmentation. In *ECCV*, 2018.

[24] Swami Sankaranarayanan, Yogesh Balaji, Arpit Jain, Ser-Nam Lim, and Rama Chellappa. Unsupervised domain adaptation for semantic segmentation with gans. In *IEEE CVPR*, 2018.

[25] Yi-Hsuan Tsai, Wei-Chih Hung, Samuel Schulter, Kihyuk Sohn, Ming-Hsuan Yang, and Manmohan Chandraker. Learning to adapt structured output space for semantic segmentation. In *IEEE CVPR*, 2018.

[26] Mei Wang and Weihong Deng. Deep visual domain adaptation: A survey. *Neurocomputing*, 312:135–153, 2018.

[27] Zhonghao Wang, Mo Yu, Yunchao Wei, Rogerior Feris, Jinjun Xiong, Wen mei Hwu, Thomas S. Huang, and Honghui Shi. Differential treatment for stuff and things: A simple unsupervised domain adaptation method for semantic segmentation. *arXiv preprint arXiv:2003.08040*, 2020.

[28] Yunchao Wei, Jiashi Feng, Xiaodan Liang, Ming-Ming Cheng, Yao Zhao, and Shuicheng Yan. Object region mining with adversarial erasing: A simple classification to semantic segmentation approach. In *IEEE CVPR*, 2017.

[29] Yunchao Wei, Xiaodan Liang, Yunpeng Chen, Xiaohui Shen, Ming-Ming Cheng, Jiashi Feng, Yao Zhao, and Shuicheng Yan. Stc: A simple to complex framework for weakly-supervised semantic segmentation. *IEEE TPAMI*, 39(11):2314–2320, 2017.

[30] Yunchao Wei, Huixin Xiao, Honghui Shi, Zequn Jie, Jiashi Feng, and Thomas S. Huang. Revisiting dilated convolution: A simple approach for weakly- and semi-supervised semantic segmentation. In *IEEE CVPR*, 2018.

[31] Zuxuan Wu, Xintong Han, Yen-Liang Lin, Mustafa Gökhan Uzunbas, Tom Goldstein, Ser-Nam Lim, and Larry S. Davis. DCAN: dual channel-wise alignment networks for unsupervised scene adaptation. In *ECCV*, 2018.

[32] Fisher Yu and Vladlen Koltun. Multi-Scale Context Aggregation by Dilated Convolutions. In *ICLR*, 2016.

[33] Yiheng Zhang, Zhaofan Qiu, Ting Yao, Dong Liu, and Tao Mei. Fully convolutional adaptation networks for semantic segmentation. In *IEEE CVPR*, 2018.

[34] Hengshuang Zhao, Jianping Shi, Xiaojuan Qi, Xiaogang Wang, and Jiaya Jia. Pyramid scene parsing network. In *IEEE CVPR*, 2017.